New Journal of Physics
The open-access journal for physics

Efficient and selective cavity-resonant excitation for single photon generation

M Kaniber[1], A Neumann, A Laucht, M F Huck, M Bichler, M-C Amann and J J Finley

Walter Schottky Institut and Physik Department, Technische Universität München, Am Coulombwall 3, D-85748 Garching, Germany
E-mail: kaniber@wsi.tum.de

New Journal of Physics **11** (2009) 013031 (9pp)
Received 15 July 2008
Published 20 January 2009
Online at http://www.njp.org/
doi:10.1088/1367-2630/11/1/013031

Abstract. We present an efficiently pumped single photon source based on single quantum dots embedded in photonic crystal nanocavities. Resonant excitation of a single quantum dot via a higher order cavity mode is shown to result in a 100× reduced optical power at the saturation onset of the photoluminescence, compared with excitation at the same frequency, after the cavity mode is shifted. We demonstrate that this excitation scheme leads to selective excitation only of quantum dots that are coupled to the cavity by comparing photoluminescence and auto-correlation spectra for the same excitation wavelength, with and without spectral resonance with the cavity mode. This excitation technique provides cleaner conditions for single photon generation and a method to select a subset of quantum dots that are spatially coupled to the nanocavity mode.

Single quantum dots (QDs) coupled to the optical modes of high quality, low mode volume solid-state nanocavities are currently attracting much interest, since they may offer a promising route towards highly efficient single photon emitters [1] for applications in quantum information science [2, 3]. However, the requirement for a high degree of spectral [4] and spatial [5] coupling between the single quantum emitter and the nanocavity mode necessitates demanding nano-fabrication techniques as well as an *in situ* spectral tuning. Recent results have shown that single QDs emitting into a two-dimensional (2D) photonic bandgap can give rise to efficient single photon generation [6]–[8]. However, the emission rate is rather low and for more demanding quantum optical applications a high degree of quantum indistinguishability [9, 10]

[1] Author to whom any correspondence should be addressed.

is needed. This necessitates the spectral and spatial coupling to the optical modes of nanoscale optical resonators. Thus, efficient methods to achieve single QD–cavity coupling are necessary. Low QD densities make it statistically very unlikely to obtain a dot that is spatially coupled to the cavity mode calling for complicated deterministic positioning of nanocavities around single dots. In contrast, higher QD densities result in higher probability for single dot–cavity coupling but degrade the purity of single photon state preparation since many dots couple to the nanocavity mode simultaneously. Therefore, cavity-resonant excitation could be exploited for realizing *selective* and *efficient* excitation of a single QD inside a nanocavity for single photon emission as proposed recently by Nomura *et al* [11, 12]. In this paper, we demonstrate an efficiently pumped single photon source based on single QDs coupled to the optical mode of a 2D photonic crystal (PC) nanocavity. By performing micro-photoluminescence (μ-PL) measurements of the same QD transition when subject to quasi-resonant excitation in the wetting layer (WL) and excitation resonant with a higher order cavity mode, we observe a striking reduction of the saturation power onset for the QD emission by a factor of 100×. Our results support the opportunity to *selectively* excite QDs which are spatially coupled to the nanocavity field by means of cavity-resonant excitation, which leads to a significantly enhanced efficiency. Furthermore, cavity-resonant excitation leads to a reduction of the complexity of the PL spectra and therefore, also to a suppression of background emission which limits the single photon state purity.

The sample studied is grown by molecular beam epitaxy and consists of the following layers grown on a semi-insulating GaAs wafer: an undoped GaAs buffer followed by a 500 nm thick $Al_{0.8}Ga_{0.2}As$ sacrificial layer and a 180 nm thick GaAs waveguide, at the midpoint of which a single layer of self-assembled $In_{0.5}Ga_{0.5}As$ QDs was incorporated. We estimated the QD density on this particular sample to approximately 5–10 dots μm^{-2}. A 2D-PC was formed by patterning a triangular array of cylindrical air holes using electron-beam lithography and reactive ion etching. The lattice constant of the PC is $a = 280$ nm and the air hole radius is $r = 0.32a$. Nanocavities were established by introducing three missing holes to form an L3 cavity [13]. Finally, free standing GaAs membranes were formed by an HF wet etching step. An overview of the different fabrication steps can be found in [14].

The sample was mounted in a liquid He-flow cryostat ($T = 15$ K) and excited by 2 ps duration pulses delivered by a Ti:sapphire laser with a repetition rate of 80 MHz. The QD μ-PL was collected via a 100× microscope objective (NA = 0.8) providing a spatial resolution of ∼700 nm, spectrally analyzed by a 0.55 m imaging monochromator and detected with a Si-based, liquid nitrogen (LN_2) cooled CCD detector. A pair of fast silicon avalanche photodiode detectors in Hanbury Brown and Twiss configuration were used for photon auto-correlation measurements.

The L3 nanocavities investigated typically show six distinct modes in μ-PL measurements spectrally distributed over more than 100 nm [14]. Due to the symmetry of the cavity the electric field mode profiles tend to be aligned either parallel or perpendicular to the axis of the line defect. Therefore, all modes exhibit a characteristic polarization that can be used to identify specific modes in the μ-PL spectra [15]. In figure 1, we present a high excitation power spectrum of two cavity modes labelled M1 ($\lambda_{M1} = 942.78$ nm) and M2 ($\lambda_{M2} = 907.01$ nm), respectively. All other higher order modes are difficult to observe in μ-PL for this low density QD sample since they have wavelengths close to or even below the WL emission. 3D calculations of the electric field distribution of the different cavity modes for an air hole radius $r = 0.32a$ (figure 1—inset) show that the fundamental and first-order cavity modes are separated by

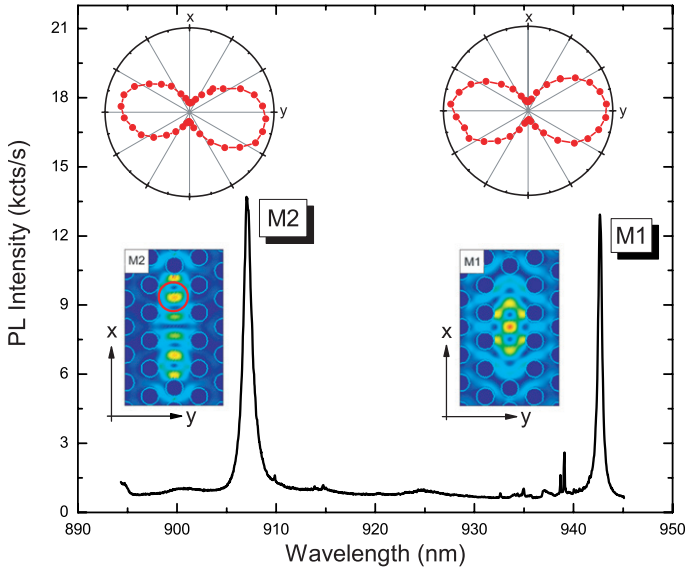

Figure 1. High-power μ-PL spectrum of the fundamental (M1) and 1st excited (M2) modes of a modified L3 cavity. Inset: corresponding 3D calculations of the E-field distribution and polarization-dependent measurements for M1 and M2.

$\sim$40 nm and exhibit similar polarizations. The measured polarization-dependent PL emission is presented in the inset of figure 1 for M1 and M2, respectively. For both cavity modes, we observe linearly polarized emission that is perpendicular (along y-axis) to the defect cavity (x-axis), in excellent agreement with the calculations of the corresponding electric field distributions of the lowest energy cavity modes of the L3 cavity. Thus, the observed cavity modes M1 and M2 are attributed to the fundamental and first-order cavity modes, respectively.

In figure 2(a), we compare μ-PL spectra recorded using quasi-resonant excitation into the 2D WL (inset—right panel) and cavity-resonant excitation via a higher energy mode (inset—left panel) for 100 μW and 1 μW, respectively. For quasi-resonant excitation (figure 2(a)—blue), the spectrum exhibits two strong QD transitions labelled $1X$ ($\lambda_{1X} = 939.18$ nm) and $1X^*$ ($\lambda_{1X^*} = 938.82$ nm) besides a couple of very weak emission features. We attribute these transitions to two different single exciton configurations of the same QD. The much broader peaks labelled M1 ($\lambda_{\mathrm{M1}} = 942.78$ nm, $Q^{\mathrm{PL}}_{\mathrm{M1}} = 2000$) and M2 ($\lambda_{\mathrm{M2}} = 907.01$ nm, $Q^{\mathrm{PL}}_{\mathrm{M2}} = 900$) are the fundamental and first excited modes of the investigated L3 cavity, respectively. By applying cavity-resonant excitation via M2 (figure 2(a)—red), the transition $1X^*$ and the weak emission features become strongly suppressed, while $1X$ and M1 dominate the spectrum. The suppression of $1X^*$ with cavity-resonant excitation and the blue shift ($E_{1X^*-1X} = 0.5$ meV) compared with $1X$ indicate that this transition very likely arises from a positively charged exciton [16]. In figure 2(b), we plot the PL intensity of $1X$ and M1 (on a double logarithmic scale) as a function of the excitation power for both WL (blue circles) and cavity-resonant excitation (red squares). With quasi-resonant excitation, we observe a linear dependence of $1X$ ($m^{\mathrm{WL}}_{1X} = 1.01$—full circles) with a saturation power $P_{\mathrm{sat}} = 100$ μW. At saturation the probability per laser pulse to create a single electron–hole pair in the QD is equal to unity. A shift of the saturation power, therefore, reflects a change of the excitation efficiency of the dot. In contrast to quasi-resonant excitation into the 2D WL, exciting $1X$ via the cavity mode M2

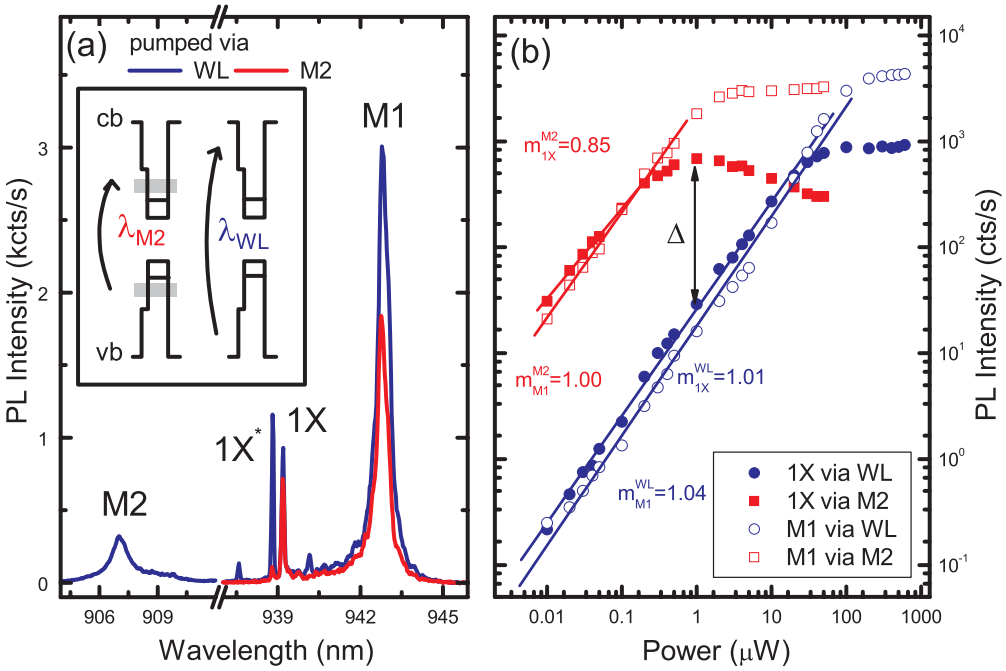

Figure 2. Panel (a) compares μ-PL spectra of the same QD with quasi-resonant excitation into the WL (blue) and with cavity-resonant excitation via M2 (red). Inset: schematic illustrations of cavity-resonant and quasi-resonant excitation. Panel (b) shows the μ-PL intensity as a function of excitation power for $1X$ (full symbols) and M1 (open symbols) with cavity-resonant excitation (red) and quasi-resonant excitation (blue).

($m_{1X}^{\mathrm{M2}} = 0.85$—full squares) results in a strongly reduced saturation power of $P_{\mathrm{sat}} = 1\,\mu$W. The reduction of the saturation power by two orders of magnitude means that we efficiently pump excitation into the dot via either (i) excited QD states (i.e. p-shell states) or (ii) the 0D–2D absorption continuum [17, 18]. Experimentally, we observe a 100× higher efficiency and this strong enhancement indicates that the QD is spatially located close to an antinode of the electric field of mode M2 as schematically indicated by the red circle in figure 1. In addition to the higher saturation level for cavity-resonant excitation, the PL intensity with cavity-resonant excitation at $1\,\mu$W is a factor $\Delta = 25\times$ higher than for quasi-resonant excitation. This shows clearly the potential for realizing an efficiently pumped single photon source by exploiting such a cavity-resonant excitation scheme.

The decrease of the $1X$ PL intensity above saturation is indicative for the existence of a non-resonant coupling mechanism between the QD transition $1X$ and the cavity mode M1 as recently published in [19]–[21]. This behaviour indicates that a mechanism exists whereby feeding of the mode by the QD emission takes place even though the dot is spectrally detuned from the cavity mode. The existence of such a non-resonant dot–cavity coupling has been unambiguously demonstrated via photon cross-correlation spectroscopy, which showed that one and the same quantum emitter can generate light at the energy of $1X$ and the spectrally detuned cavity mode M1 [21]. The underlying mechanism that is responsible for this non-resonant coupling has not yet been unambiguously identified, although the authors of [21] suggested that it may be due to cavity enhanced shake-up like processes in the emission from multiple charged

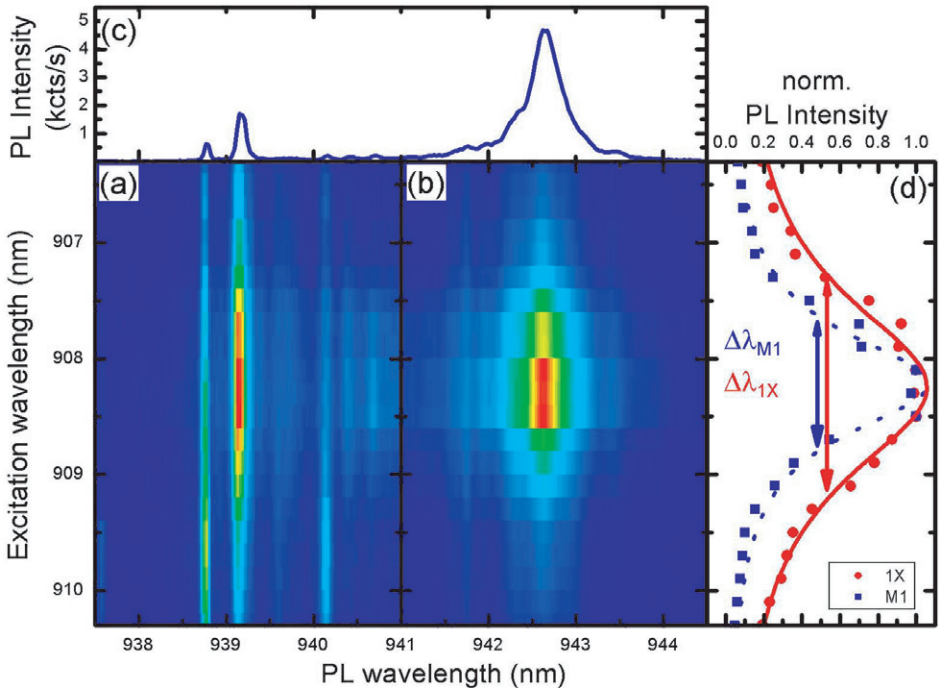

Figure 3. (a) and (b) MPLE spectra of $1X$ and M1, respectively. (c) μ-PL spectrum of $1X$ and M2 at resonance ($\lambda_{res} = 908.25$ nm). (d) PLE spectra of $1X$ (circles) and M1 (squares).

QDs [22]. Evidence for this non-resonant coupling is observed in the power dependence of the cavity mode M1 recorded using cavity-resonant excitation via M2 (open squares) in figure 2(b). The intensity of M1 in the saturation regime increases while the $1X$ intensity reduces. This effect is not unique to cavity-resonant excitation and should also occur for quasi-resonant excitation. However, it is more readily observed for cavity-resonant excitation due to the reduced excitation power at the onset of saturation.

Excitation via a higher order cavity mode enhances the absorption of the incident light at the high electric field regions inside the defect cavity [11, 23]. This enhancement effectively reduces the excited region of the sample due to concentration of the excitation power inside the cavity region. Therefore, we expect that excitation via a higher energy cavity mode should enable us to selectively excite QDs that are spatially coupled to an electric field maximum of that specific mode. To check this expectation we performed multichannel photoluminescence excitation (MPLE) measurements in which we scanned the excitation wavelength through the higher order cavity mode M2 from $\lambda_{exc} = 906.3$ nm to 910.3 nm and simultaneously recorded the PL spectra around the lower energy mode M1. The result of these measurements are shown in figures 3(a) and (b), where the detection and excitation wavelengths are plotted on the x- and y-axis, respectively, and the PL intensity is encoded in false colour. We observe a common maximum in the intensity of both $1X$ and M1 when exciting spectrally in resonance with the higher energy mode M2 at $\lambda_{exc} = \lambda_{M2} = 908.25$ nm.[2] This observation indicates that the

[2] The slight offset between of λ_{M2} in PLE measurements compared to PL measurements is due to an offset of the excitation laser frequency.

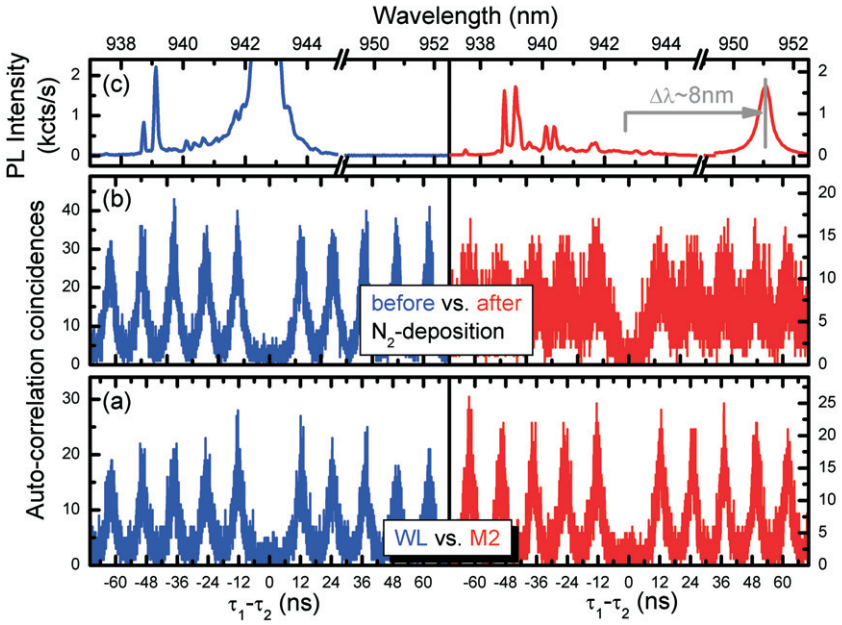

Figure 4. Panel (a) compares auto-correlation spectra recorded on $1X$ with quasi-resonant excitation (left panel) and cavity-resonant excitation (right panel). Panel (b) compares auto-correlation spectra recorded on $1X$ before (left panel) and after (right panel) N_2-deposition for constant excitation wavelength. Panel (c) compares μ-PL spectra before (left panel) and after (right panel) N_2-deposition.

QD transition is spatially coupled to the cavity field maximum of the mode M2. Moreover, it demonstrates that the excitation pumped into the cavity at λ_{M2} is directly transferred to the particular QD transition of interest. For comparison, in panel (c) we plot a PL spectrum recorded at $\lambda_{exc} = \lambda_{M2}$. In figure 3(d), we present the normalized PL intensity of $1X$ (circles) and M1 (squares) as a function of the excitation wavelength. Both curves should, in principle, reflect the spectral form of cavity mode M2 via which the system has been excited. By fitting the data points for the lower energy mode M1, we obtain a quality factor of $Q_{M2}^{\text{via M1}} = 850$, which is in very good agreement with the value directly obtained for M2 in the PL studies discussed in figure 2. However, the quality factor obtained from the MPLE spectrum detected on the $1X$ transition ($Q_{M2}^{\text{via } 1X} = 470$) is lower than that measured by PL since this measurement has been conducted with an excitation power in the saturation regime of $1X$, where the PL intensity decreases as shown in figure 2(b).

To test the feasibility of the cavity-resonant excitation scheme for realizing an efficiently pumped single photon source, we performed photon auto-correlation spectroscopy while probing the photon statistics of the $1X$ transition. In figure 4(a), we compare auto-correlation measurements recorded from $1X$ with quasi-resonant excitation into the WL (left panel) and cavity-resonant excitation via M2 (right panel). For both excitation schemes we chose optical powers such that the excitation level of the dot was nominally equivalent, near the PL saturation level. By reference to figure 2(b), this is 100 μW and 1 μW for quasi-resonant and cavity-resonant excitation, respectively. In both cases, we recorded auto-correlation traces for an integration time $t = 5000$ s and obtained a strong suppression of the multi-photon emission probability to $\sim$25% of a Poissonian source of equal intensity for both quasi-resonant and

cavity-resonant excitation. Although we observe qualitatively similar results for both excitation schemes, it is important to note that we reduced the excitation power by a factor of 100× when exciting via the higher order mode M2, as compared with exciting into the WL. This clearly underscores the advantage of cavity mode pumping for optimizing the ratio of PL saturation intensity to incident optical power.

Direct comparison of the excitation schemes at two different spectral positions, and consequently different optical absorption coefficients, does not unambiguously prove the concept of cavity-resonant pumping. A local maximum of the absorption coefficient (e.g. due to excited QD states) at λ_{M2} would also explain the pronounced decrease in saturation power. However, a controlled deposition of molecular nitrogen N_2 on to the sample surface [24], enables us to controllably detune the cavity modes from their original spectral positions by adsorption into the PC at low temperatures. This allows us to test if the reduction in excitation power needed to generate clean single photon emission is really caused by the existence of a cavity mode (M2) or simply due to the difference in optical absorption coefficients for both excitation schemes. Thus, we performed auto-correlation measurements on $1X$ for exactly the same excitation conditions ($\lambda_{exc} = \lambda_{M2}$) *before* and *after* the N_2-induced shift of M2. The results presented in figure 4(b) were obtained for excitation before (left panel) and after (right panel) the N_2-deposition and same integration time $t = 7200$ s. Qualitatively very similar results are obtained for both measurements regarding the total coincidence counts and the suppression of multiphoton emission probability. The enhanced background between two adjacent peaks in the auto-correlation spectrum after the N_2-deposition (b—right) is due to the longer lifetime of the $1X$ transition since the mode M1 is also further detuned from $1X$ [21]. This result confirms that the reduction of the excitation power by two orders of magnitude is, indeed, related to the existence of the cavity mode at λ_{M2} since the onset of saturation was found to shift from 1 μW (before N_2-deposition) to 100 μW (after N_2-deposition) (data not shown here). The corresponding PL spectra presented in figure 4(c), clarify that M1 has indeed shifted by $\sim$8 nm towards longer wavelength after the injection of N_2. Furthermore, the PL spectrum after the deposition becomes clearly much more complicated indicating that the excitation is *not* as selectively directed towards a single QD state as it was before the deposition. Thus, cavity-resonant pumping effectively suppresses emission of QDs which are spatially more weakly coupled to the cavity M2. We conclude therefore, that cavity-resonant pumping leads to clear *selective* excitation of dots that are spatially coupled to the electric field maximum of the cavity mode M2.

In order to realize efficient generation of indistinguishable single photons, one needs to spectrally and spatially couple a single QD to a nanocavity mode. The concept of cavity-resonant excitation can easily be extended to such a spectrally and spatially coupled dot–cavity system as illustrated schematically in figure 5. The single QD (blue) is spectrally in resonance with the fundamental mode M1 of the nanocavity and spatially located at an antinode of the corresponding electric field profile, as indicated by the red circle in figure 5 (inset). To apply cavity-resonant excitation, the second cavity mode needs to have a common antinode of the electric field, and therefore, one cannot use the first-order cavity mode M2 (cf electric field distributions in figure 1). However, a suitable cavity mode in an L3 cavity would be the mode M4 whose electric field profile is also plotted as inset in figure 5. Mode M4 can either be spectrally in resonance with the p-shell states of the considered QD or with continuum crossed-transitions [17, 18]. This combination of cavity-resonant excitation and Purcell enhanced emission would result in a single photon source that is highly efficient both in excitation and emission.

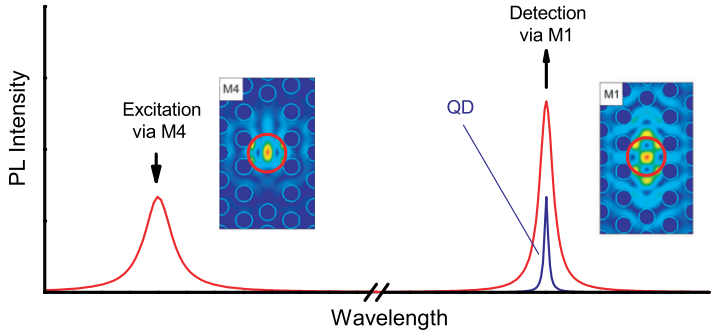

Figure 5. Schematic illustration of the cavity-resonant excitation scheme for a spectrally and spatially coupled dot–cavity system.

In summary, we have demonstrated the practicability of a cavity-resonant excitation scheme for an efficiently pumped single photon source based on QDs coupled to PC nanocavities. Excitation via a higher order cavity mode was shown to result in comparable PL intensities of the QD and multiphoton emission probabilities, as compared with non-resonant excitation, while the necessary optical power needed to generate the same excitation level in the dot is reduced by a factor up to 100×. Furthermore, we showed that this new excitation scheme leads to suppression of the emission from QDs which are spatially decoupled from the electric field inside the cavity allowing for much more direct excitation of a specific QD state. We also suggested how this concept can easily be applied to a spectrally and spatially coupled QD–cavity system. In addition to efficient single photon emission in this type of system [6], we believe that this technique may also enable new perspectives on the route towards efficient optical pumping of a single photon source, since it provides a method for clean and efficient quantum state population.

Acknowledgments

We acknowledge financial support of the Deutsche Forschungsgemeinschaft via the Sonderforschungsbereich 631, Teilprojekt B3 and the German Excellence Initiative via the 'Nanosystems Initiative Munich (NIM)'.

References

[1] Michler P, Kiraz A, Becher C, Schoenfeld W V, Petroff P M, Zhang L, Hu E and Imamoğlu A 2000 *Science* **290** 2282
[2] Knill E, Laflamme R and Milburn G J 2001 *Nature* **409** 46
[3] Gisin N, Ribordy G, Tittel W and Hugo Zbinden 2002 *Rev. Mod. Phys.* **74** 145
[4] Hofbauer F, Grimminger S, Angele J, Böhm G, Meyer R, Amann M-C and Finley J J 2007 *Appl. Phys. Lett.* **91** 201111
[5] Badolato A, Hennesssy K, Atatüre M, Dreiser J, Hu E, Petroff P M and Imamoğlu A 2005 *Science* **308** 1158
[6] Kaniber M, Laucht A, Hürlimann T, Bichler M, Meyer R, Amann M-C and Finley J J 2008 *Phys. Rev.* B **77** 073312
[7] Englund D, Fattal D, Waks E, Solomon G, Zhang B, Nakaoka T, Arakawa Y, Yamamoto Y and Vučkovic J 2005 *Phys. Rev. Lett.* **95** 013904

[8] Chang W-H, Chen W-Y, Chang H-S, Hsieh T-P, Chyi J-I and Hsu T-M 2006 *Phys. Rev. Lett* **96** 117401
[9] Santori C, Fattal D, Vučkovic J, Solomon G S and Yamamoto Y 2002 *Nature* **419** 594
[10] Laurant S, Varoutsis S, Le Gratiet L, Lemaître A, Sagnes I, Raineri F, Levenson A, Robert-Philip I and Abram I 2005 *Appl. Phys. Lett.* **87** 163107
[11] Nomura M, Iwamoto S, Yang T, Ishida S and Arakawa Y 2006 *Appl. Phys. Lett.* **89** 241124
[12] Nomura M, Iwamoto S, Nishioka M, Ishida S and Arakawa Y 2006 *Appl. Phys. Lett.* **89** 161111
[13] Akahane Y, Asano T, Song B-S and Noda S 2003 *Nature* **425** 944
[14] Kress A, Hofbauer F, Reinelt N, Kaniber M, Bichler M, Schuh D, Böhm G and Finley J J 2005 *Proc. SPIE—Int. Soc. Opt. Eng.* **5733** 114–24
[15] Chalcraft A R A *et al* 2007 *Appl. Phys. Lett.* **90** 241117
[16] Finley J J, Ashmore A D, Lematre A, Mowbray D J, Skolnick M S, Itskevich I E, Maksym P A, Hopkinson M and Krauss T F 2001 *Phys. Rev.* B **63** 073307
[17] Vasanelli A, Ferreira R and Bastard G 2002 *Phys. Rev. Lett.* **89** 216804
[18] Oulton R, Finley J J, Tartakovskii A I, Mowbray D J, Skolnick M S, Hopkinson M, Vasanelli A, Ferreira R and Bastard G 2003 *Phys. Rev.* B **68** 235301
[19] Hennessy K, Badolato A, Winger M, Gerace D, Atatüre M, Gulde S, Fält S, Hu E L and Imamoğlu A 2007 *Nature* **445** 896
[20] Press D, Götzinger S, Reitzenstein S, Hofmann C, Löffler A, Kamp M, Forchel A and Yamamoto Y 2007 *Phys. Rev. Lett.* **98** 117402
[21] Kaniber M, Laucht A, Neumann A, Villas-Bôas J M, Bichler M, Amann M-C and Finley J J 2008 *Phys. Rev.* B **77** 161303
[22] Karrai K, Warburton R J, Schulhauser C, Hoğele A, Urbaszek B, McGhee E J, Govorov A O, Garcia J M, Gerardot B D and Petroff P M 2004 *Nature* **427** 135
[23] Oulton R *et al* 2007 *Opt. Express* **15** 17221
[24] Mosor S, Hendrickson J, Richards B C, Sweet J, Khitrova G, Gibss H M, Yoshie T, Scherer A, Shchekin O B and Deppe D G 2005 *Appl. Phys. Lett.* **87** 141105